Material Science and Applied Chemistry
doi: 10.7250/msac.2013.009
2013 / 28

The Study of Magnesium Substitution Effect on Physicochemical Properties of Hydroxyapatite

Liga Stipniece[1], Kristine Salma-Ancane[2], Dmitrijs Jakovlevs[3], Natalija Borodajenko[4], Liga Berzina-Cimdina[5]
[1-5]*Riga Technical University*

Abstract. **In the present study, pure and Mg-substituted hydroxyapatite powders made up of needle-like and plate-like particles, respectively, have been synthesized by wet chemical precipitation of CaO, MgO and H_3PO_4. The influence of different amounts of MgO addition into synthesis media on properties of as-synthesized and sintered powders has been evaluated.**

Through the phase and chemical composition analysis it has been determined that the prepared powders contain various amounts of Mg (in the range between 0.21–4.72 wt%). The substitution of Mg promoted the decomposition of hydroxyapatite to β-tricalcium phosphate.

Keywords: **bioceramics, hydroxyapatite, magnesium, wet chemical precipitation**

I. Introduction

Hydroxyapatite (HAp, chemical formula $Ca_{10}(PO_4)_6(OH)_2$) has attracted the attention of researchers over the past thirty years as an implant material because of its excellent biocompability and bioactivity. It is commonly the material of choice for the fabrication of dense and porous bioceramics [1]. All properties of HAp, including bioactivity, biocompatibility and solubility can be tailored within a wide range by controlling qualitatively and quantitatively ions substituted for Ca^{2+}, PO_4^{3-} and OH^- in the HAp lattice structure [2].

Magnesium (Mg) is known as one of the cationic substitutes for calcium (Ca) in the HAp lattice structure [3]. Magnesium-substituted HAp (Mg-HAp) can be expressed by a simplified chemical formula: $Ca_{10-x}Mg_x(PO_4)_6(OH)_2$. Mg is also one of the predominant substitutes for Ca in biological apatite (enamel, dentin, and bone contain 0.44 wt%, 1.23 wt% and 0.72 wt% of Mg, respectively) [3-7]. Accordingly, Mg-HAp materials are expected to have excellent biocompability and properties that can be favourably compared to those of hard tissues [7]. *Caccioti et al.* and *Kim et al*. have found through their studies that the presence of Mg ions within HAp lattice affects its crystallization in solution, its thermal stability, promotes the formation of β-tricalcium phosphate (β-TCP) during thermal treatment, thus forming biphasic calcium phosphates (BCP) [5,8]. According to the literature, the replacement of Ca by Mg in HAp is limited. This is related to the size differences between Mg^{2+} and Ca^{2+} (~0.28 Å difference in radius according to the Pauling scale) [9]. The maximal amount of Mg substituting for Ca varies in previous research reports. For example, *Mayer et al.* [10] precipitated HAp containing up to 1.5 wt% of Mg. *Fadeev et al.* [11] reported that ~10 wt% was the maximal amount of Mg ions that could be successfully incorporated into HAp structure replacing Ca ions. *Riman et al*. [12] even reported stable, phase-pure Mg-substituted crystalline HAp containing from ~2.0 to ~29 wt% Mg obtained through the mechanochemical–hydrothermal technique, wherein at least 75 wt% of Mg substituted for Ca ions in the HAp lattice structure. The changes of crystal structure have a direct impact on the properties of Mg-HAp, compared to their non-substituted analogues [3,11]. Increasing concentration of Mg in HAp has the following effects on its properties: a) gradual decrease in crystallinity; b) increase in HPO_4 incorporation, and c) increase in the extent of dissolution [13]. Mg is associated with mineralization of calcified tissues and indirectly influences mineral metabolism [6]. It becomes possible to tailor the physicochemical properties of HAp, as well as its biocompability and bioactivity, by controlling the Mg substitution of the HAp lattice structure [14].

The purpose of the present research has been to study the effect of partial Mg substitution for Ca on the structure and properties of HAp synthesized through wet chemical precipitation involving calcium oxide (CaO), magnesia (MgO) and orthophosphoric acid (H_3PO_4) precursors.

II. Materials and Methods

Pure and Mg-HAp powders containing various contents of Mg were synthesized from CaO (*Riedel-de-Haën®*), MgO (*ES/Scharlau*) and H_3PO_4 (*Sigma-Aldrich*) through wet chemical precipitation, according to the scheme shown in Fig.1.

The starting slurries were obtained through "lime slaking" processes by dissolving CaO or CaO/MgO powders (to obtain pure or Mg substituted products, respectively) into deionized H_2O, and completely homogenized by a planetary ball milling (*FRITCH planetary mill PULVERISETTE 5*) at 300 rpm for 40 min. MgO contents in synthesis media ranged between 0.1–20.0 wt% in respect to the total amount of mixture containing CaO and MgO.

Precipitation reaction was carried out in a laboratory reactor (*IKA EUROSTAR Power Control-Visc P7*), where an aqueous solution of 2.0 M H_3PO_4 was added to $Ca(OH)_2$ or $Mg(OH)_2/Ca(OH)_2$ suspension at a slow addition rate (~0.75 ml/min) using titration equipment (*TITRONIC*) under vigorous stirring. The temperature of synthesis media was maintained constant (45 °C) and the pH was continuously monitored and adjusted to 9.0 during synthesis by adding 2.0 M H_3PO_4, and stabilized for 1 h.

After synthesis the precipitates were aged in mother liquor for ~20 h at ambient temperature, filtered and dried at 105 °C

for ~20 h. The powders were ground and analysed (as-synthesized powders). Subsequent sintering of as-synthesized powders followed in an electrically heated furnace (*Nabertherm LHT 08/17*) in air atmosphere at 1100 °C (sintered powders).

Comprehensive characterization techniques, including Fourier transform infrared spectrometer (FT-IR) – *Varian 800*, *PANalitical X'pert PRO* X-ray powder diffractometer (XRD), differential thermal analyzer (DTA) *BÄHR DTA703*, heating microscope (HM) *Hesse Instruments Heating Microscope – EM 201 (HT-16 (1600/80))*, and field emission scanning electron microscopy (FE-SEM) *Tescan Mira/LMU* and energy dispersive X-ray spectroscopy (FE-SEM/EDS) (*Inca Energy 350*), were used to investigate the effect of Mg substitution on phase composition, crystallinity, thermal stability, sintering behaviour, morphology, microstructure and chemical composition, respectively, of as-synthesized and sintered products.

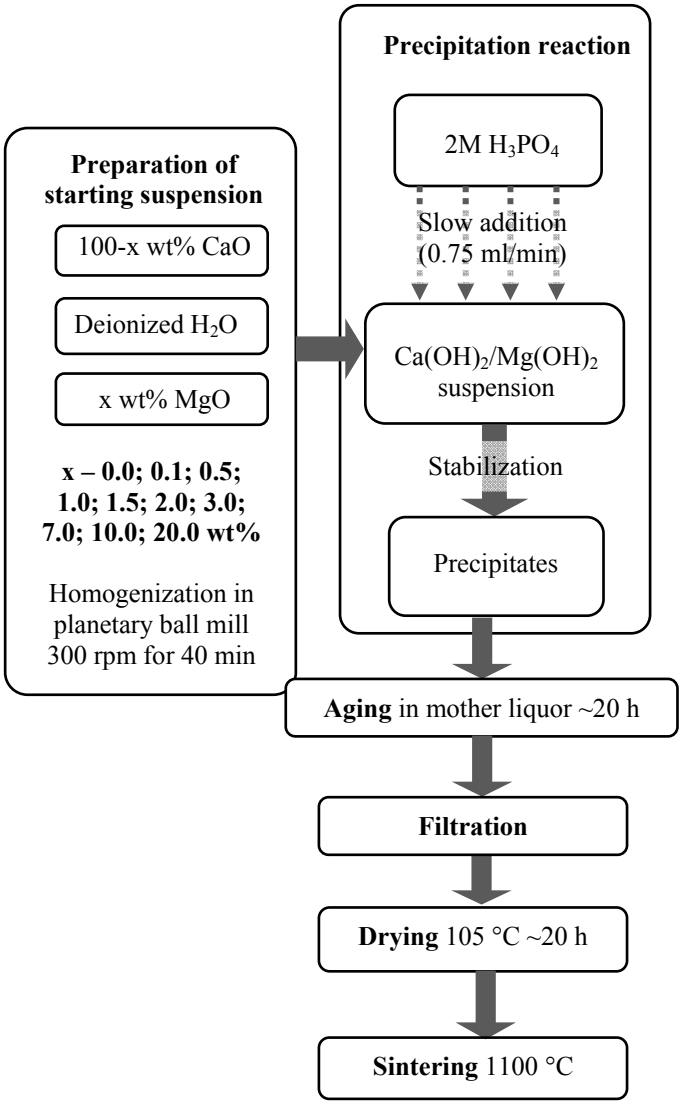

Fig. 1. Technological scheme of preparation of HAp and Mg-HAp powders

The mean sizes of crystallites of as-synthesized HAp and Mg-HAp products were calculated according to the Scherrer's equation:

$$D = k \cdot \lambda / (FWHM \cdot \cos\theta) \quad (1)$$

In order to calculate the mean sizes of crystallites of as-synthesized powders, the peak of XRD patterns of as-synthesized product was chosen at 25.9° 2θ, since it was isolated, *i.e.*, did not overlap with other diffraction peaks. In the case of sintered powders, to calculate the mean sizes of crystallites the peaks of XRD patterns of sintered product were chosen at 25.9° 2θ and 32.9° 2θ, the FWHM values of which represented length and width of crystallites, respectively [15].

III. Results and Discussion

A. Chemical Composition

FE-SEM/EDS measurements show the presence of Ca, P, Mg and O in both HAp and Mg-HAp samples. Powders prepared with CaO and H_3PO_4 without extra MgO addition in the starting suspension contain 0.21wt% of Mg. This Mg content results from impurities in commercial CaO. In general, Mg content in synthesis products increased proportionally with the amount of MgO in the starting slurry between 0.21 and 4.72 wt% (see Table 1 and Fig. 2). It is likely to achieve concentrations of Mg substitutions (*i.e.*, 0.52, 0.64 and 0.83 wt%) in HAp resembled to those of bone mineral by adding 1.5, 2.0 and 3.0 wt% of MgO, respectively, into synthesis media.

TABLE 1

Mg Concentration in Synthesis Products Sintered at 1100 °C for 1 h Determined by FE-SEM/EDs Analysis

Sample	Mg concentration, wt%
HAp	0.21 ± 0.03
0.1_Mg-HAp	0.21 ± 0.06
0.5_Mg-HAp	0.31 ± 0.09
1.0_Mg-HAp	0.43 ± 0.10
1.5_Mg-HAp	0.52 ± 0.29
2.0_Mg-HAp	0.64 ± 0.08
3.0_Mg-HAp	0.83 ± 0.21
7.0_Mg-HAp	1.50 ± 0.45
10.0_Mg-HAp	2.11 ± 0.15
20.0_Mg-HAp	4.72 ± 1.24

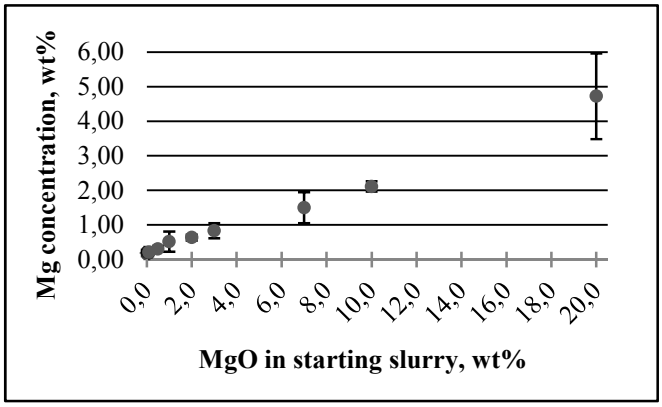

Fig. 2. Mg concentration in HAp and Mg-HAp powders (0.1; 0.5, 1.0; 1.5, 2.0, 3.0; 7.0, 10.0, 20.0 wt% MgO) sintered at 1100 °C for 1 h determined by FE-SEM/EDS analysis

B. Phase Composition, Cristallinity

XRD patterns of as-synthesized HAp and Mg-HAp powders are compared in Fig. 3. Identification of the crystalline phases was carried out using the X-ray diffraction data of existing clean phases from the *American Mineralogist Crystal Structure Database* (AMCDS). All the as-synthesized powders had a low degree of crystallinity as evidenced by XRD patterns with relatively broad and low intensity XRD peaks, which were attributed to small crystallite size characteristic of the apatite phase. No observable differences of crystallinity in XRD patterns of as-synthesized HAp and Mg-HAp were detected. It was observed that in our case incorporation of Mg into HAp had only a minor influence on the crystal dimensions of as-synthesized HAp and Mg-HAp. Thus, it can be concluded that Mg ions recruited to HAp structure cause insignificant deformations of crystallites. It was evident by the absence of unreacted MgO (*AMCDS #0004683*) or presence of $Mg(OH)_2$ (*AMCDS #0002434*), and magnesium phosphates (MgP) that could be formed as by-products of synthesis (*i.e.*, newberyite ($MgHPO_4*3H_2O$; *AMCSD #0009693*), farringtonite ($Mg_3(PO_4)_2$; *AMCDS #0011901*), bobierrite and baricite ($Mg_3(PO_4)_2*8(H_2O)$; *AMCDS #0001049*)) in any of Mg-HAp patterns, where all Mg was incorporated into Mg-HAp.

After sintering at 1100 °C for 1 h the obtained XRD patterns of HAp and Mg-HAp are reported in Fig. 4 and Fig. 5. The XRD analyses show that products with low concentrations of Mg, *i.e.*, HAp, 0.1_Mg-HAp, 0.5_Mg-HAp, 1.0_Mg-HAp, 1.5_Mg-HAp and 2.0_Mg-HAp, contain a single crystalline phase – HAp (*AMCDS #0001257*) (see Fig. 4). When concentration of Mg in synthesis products increased (between 0.83–4.72 wt%), characteristic peaks of HAp and β-TCP appeared in captured powder X-ray diffraction patterns suggestive of existence of β-TCP and/or whitlockite (Mg-β-TCP, Mg-substituted β-TCP) in these samples (see Fig. 5). To identify phases 2θ the values reported in *AMCSD #0004624* and *AMCSD #0013351* for synthetic β-tricalcium phosphate and whitlockite were used, respectively.

Incorporation of Mg led to a gradual transformation of HAp in whitlockite depending on Mg content, which was also confirmed by the DTA and HM data.

C. Molecular Composition

The FT-IR spectra of as-synthesized HAp and Mg-HAp present the characteristic vibrational bands of typical partially carbonated and hydrated apatite. FT-IR spectra of sintered samples differ significantly from the FT-IR spectra of as-synthesized samples. All spectra have intensive characteristic bands of HAp originating from vibration of phosphates groups [PO_4] and bands corresponding to stretching and vibrational modes of the hydroxyl groups [OH]. Thus, increase in Mg content of sintered samples observed [PO_4] characteristic absorption band broadening and splitting. In the case of 7.0_Mg-Hap, 10.0_Mg-HAp and 20.0_Mg-HAp extra peaks were detected. These bands can be ascribed to the [PO_4] group vibration modes characteristic of whitlockite. By increasing content of Mg in HAp structure, extra peaks become more intense (see Fig. 6).

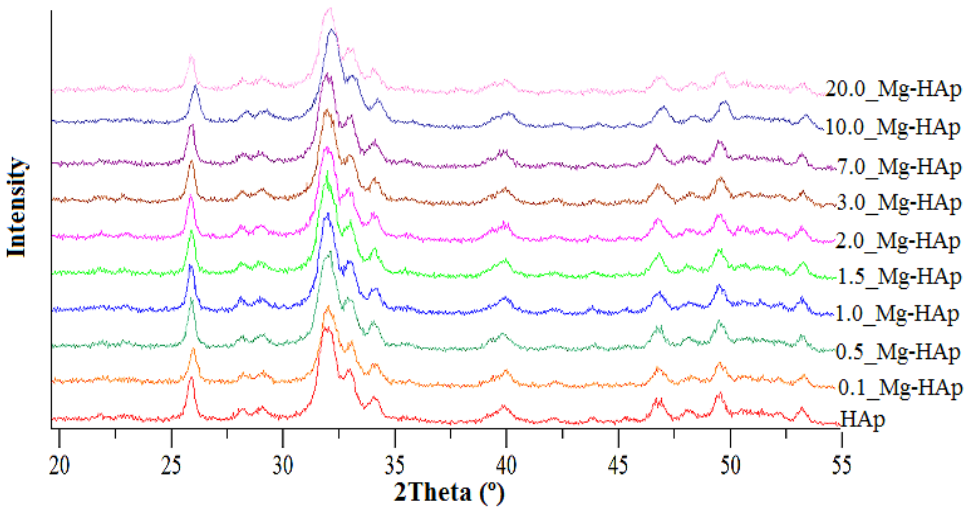

Fig. 3. XRD patterns of as-synthesized HAp and Mg-HAp powders dried at 105 °C for 20 h

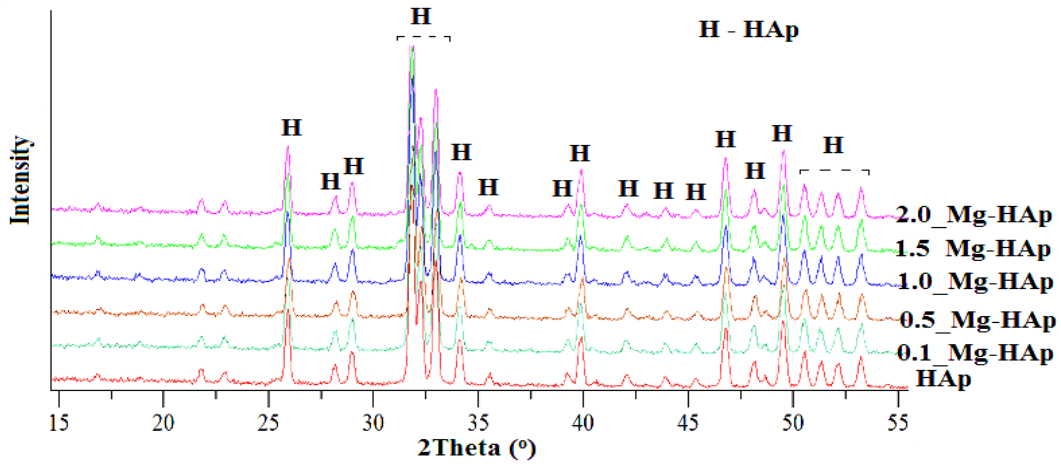

Fig. 4. XRD patterns of sintered HAp and Mg-HAp (HAp, 0.1_Mg-HAp, 0.5_Mg-HAp, 1.0_Mg-HAp, 1.5_Mg-HAp, 2.0_Mg-HAp) powders at 1100 °C for 1 h

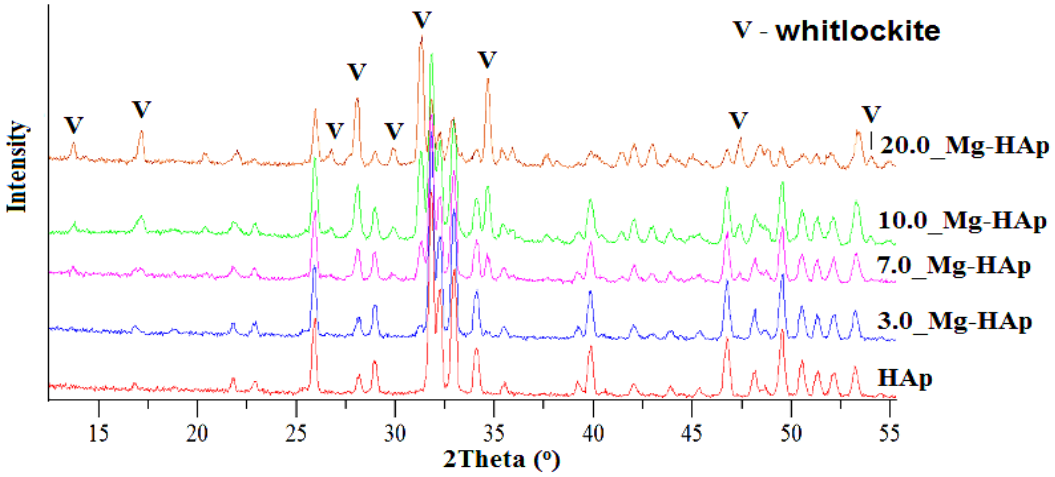

Fig. 5. XRD patterns of sintered Mg-HAp (3.0_Mg-HAp, 7.0_Mg-HAp, 10.0_Mg-HAp, 20.0_Mg-HAp) powders at 1100 °C for 1 h

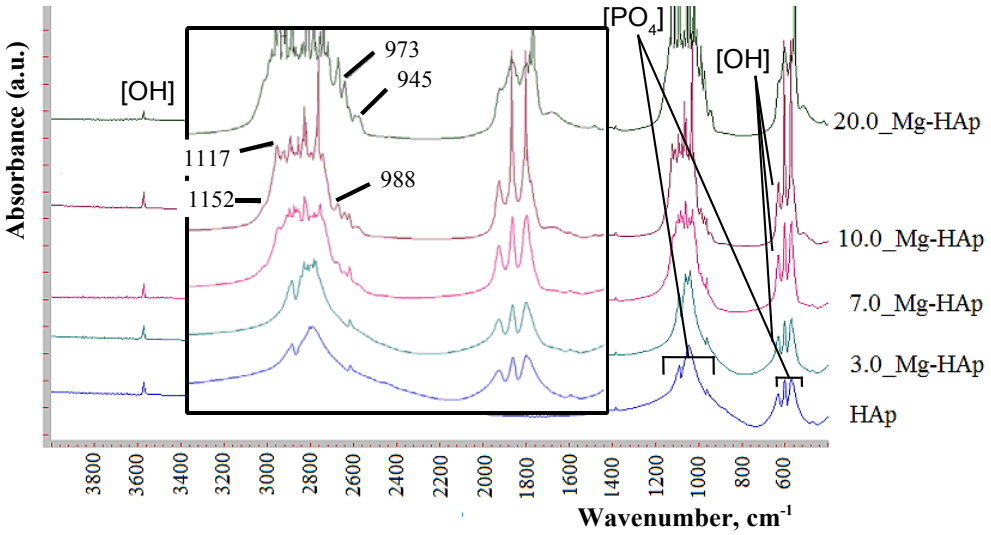

Fig. 6. FT-IR spectra of sintered HAp and Mg-HAp powders at 1100 °C for 1 h [16]

D. Thermal Stability and Sintering Behaviour

DTA analysis (Fig. 7) up to 1400 °C of HAp and 10_Mg-HAp powders confirmed the results of XRD analyses. Endothermic effect in the temperature region from 50–150 °C was due to the removal of physically adsorbed H_2O and CO_2. Pure HAp did not show any other endothermic peaks up to 1400 °C. In the case of 10.0_Mg-HAp, the DTA curve showed some distortions in the temperature region from 700 to 1150 °C. Thus, this region of DTA curve could be caused due to the decomposition of the Mg-HAp to whitlockite phase. This effect was also observed in the studies of HM (Fig. 8).

The sintering process of Mg-HAp bioceramics started at temperature ~680–750 °C. Linear shrinkage at the temperature range of 650–1000 °C pointed to the beginning of phase decomposition; this process overlapped with the beginning of compaction of bioceramics.

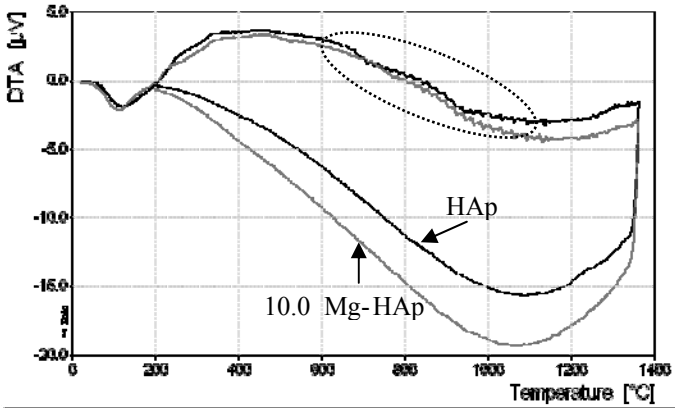

Fig. 7. DTA curves of HAp and 10.0_Mg-HAp products

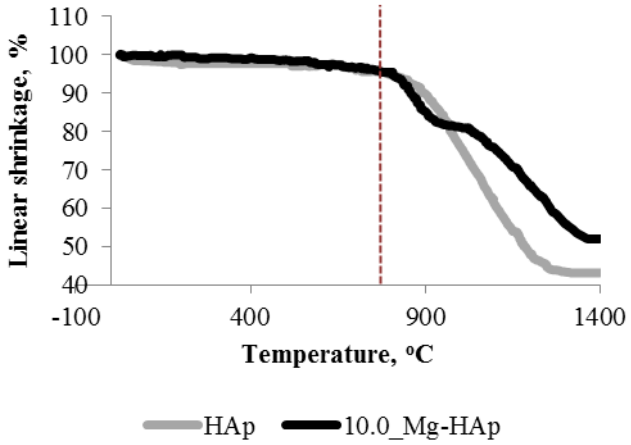

Fig. 8. Thermal shrinkage of HAp and 10.0_Mg-HAp samples

E. Morphology and Microstructure

The samples were collected in the form of suspension after the stabilization period of ~1 h to investigate the morphology of as-synthesized HAp and Mg-HAp powders. FE-SEM microphotograph (Fig. 9) of as-synthesized pure HAp shows typical nanosized needle-like crystallite morphology with homogenous, thin, elongated (~150-200 nm) crystallites. Morphologies of as-synthesized Mg-HAp suspensions show different shapes and sizes of crystallites. Mg-HAp suspensions after synthesis show the plate-like crystallite agglomerate morphology. As Mg content in the synthesis products increased (especially in the case of samples 10.0_Mg-HAp and 20.0_Mg-HAp), crystallites become thinner and finer and more agglomerated. Since crystallites of as-synthesized HAp and Mg-HAp tend to agglomerate, it is impossible to determine the crystallite sizes through the analysis of the FE-SEM images, because it is possible to distinguish only primary agglomerates of crystallites.

However, calculations using the Scherrer's equation showed that the mean sizes of crystallites of as-synthesized HAp and Mg-HAp were in the range between ~20–25 nm.

The similar values of mean sizes of crystallites for as-synthesized powders containing different amounts of Mg imply that in our case the incorporation of Mg ions probably had only a minor influence on crystal dimensions.

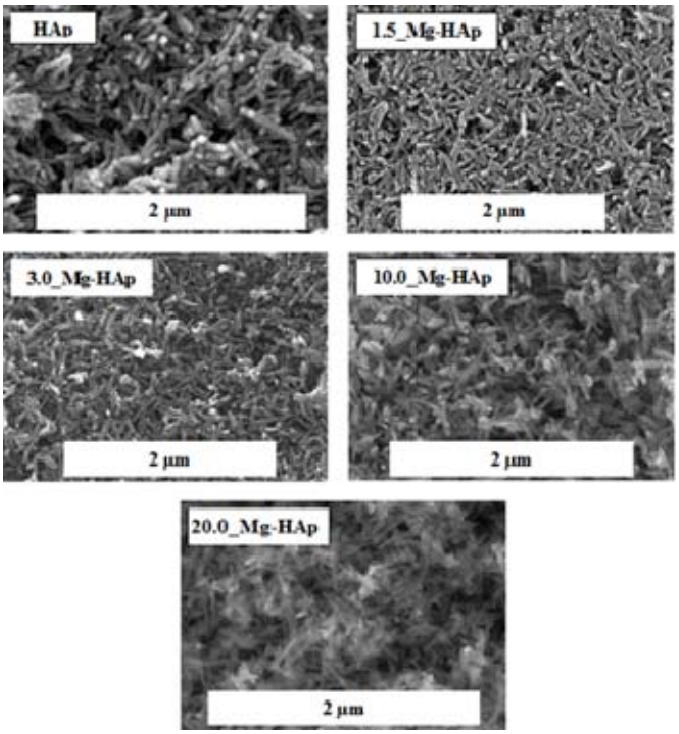

Fig. 9. FE-SEM microphotographs of as-synthesized powder suspensions dried at 105 °C for 20 h

The results of FE-SEM investigation of the microstructure of sintered pure and Mg-HAp bioceramics showed that the incorporation of Mg into HAp structure increased the densification of HAp bioceramics. It is evident that an increase in Mg content in bioceramic samples induces the formation of elongate grains. After the thermal treatment, the calculated values of length and width of crystallites of HAp and Mg-HAp products were ~30–40 nm, thus, indicating that the sintering at 1100 °C for 1h induced the rounding and compression of crystallites, being a characteristic of HAp sintering process. It was observed that in the case of 7.0_Mg-HAp and 20.0_Mg-Hap, the microstructure was more microporous than that of other Mg-substituted bioceramic

structures due to the presence of the secondary phase – whitlockite (Fig. 10).

All pure-phase Mg-HAp bioceramics showed good densification with respect to HAp. Porosity and bulk density of HAp and Mg-HAp bioceramics after thermal treatment were also determined using a method based on Archimedes' principle, and the results confirm FE-SEM microphotographs (Fig. 11).

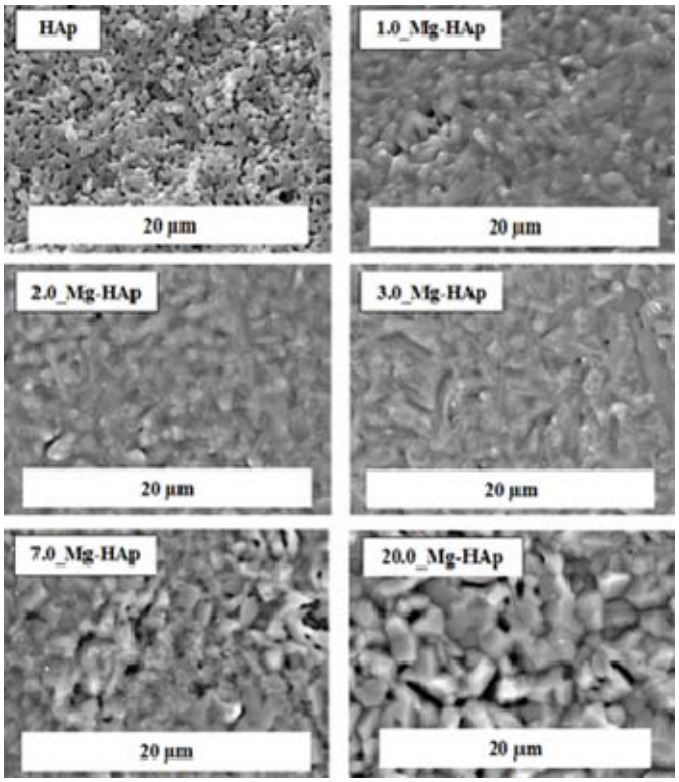

Fig. 10. FE-SEM microphotographs of surface microstructures of HAp, Mg-HAp bioceramics sintered at 1100 °C for 1 h

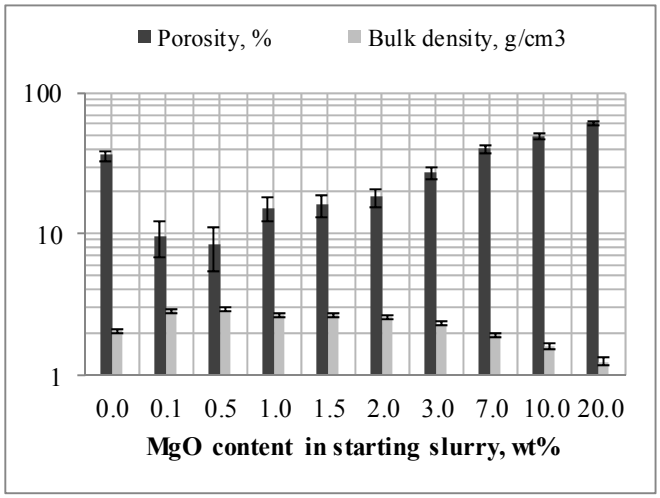

Fig. 11. HAp (0.0 wt% MgO) and Mg-HAp (0.1–20.0 wt% MgO) bioceramics total porosity and bulk density

IV. Conclusions

Mg-substituted hydroxyapatite with variable amount of Mg (0.21–4.72 wt%) incorporated into the structure has been synthesized by modified wet chemical precipitation. After the synthesis and thermal treatment, the obtained X-ray diffraction analysis has not shown the presence of $Mg(OH)_2$ and MgO in Mg-substituted hydroxyapatite products, which indicates complete Mg ion incorporation into the hydroxyapatite structure. Mg concentration of Mg-substituted hydroxyapatite products increases with an increase in the MgO content in $Ca(OH)_2/Mg(OH)_2$ suspension. Mg-substituted hydroxyapatite thermal stability decreases by increasing the content of Mg into hydroxyapatite products; Mg-substituted hydroxyapatite partial transformation to Mg-substituted β-tricalcium phosphate or whitlockite occurred. The incorporation of Mg into hydroxyapatite structure significantly affects its crystallite morphology and microstructure of bioceramics.

Acknowledgements

The research has been supported by the Latvian State Research Programme "Development of Innovative Multifunctional Materials, Signal Processing and Information Technology for Competitive Science-intensive Products" within the framework of project No. 4 "New Materials and Technologies for Evaluating Biological Tissue, and Replace".

References

1. **Albrektsson, T., Johansson, C**., Osteoinduction, osteoconduction and osseointegration. *Eur. Spine J.*, 2001, vol. 10, p. S96-S101. http://dx.doi.org/10.1007/s005860100282
2. **Boanini, E., Gazzano, M., Bigi, A.,** Ionic substitutions in calcium phosphates synthesized at low temperature, *Acta Biomaterialia*, 2010, vol. 6, p. 1882.-1894.
3. **Landi, E., Logroscino, G., Proietti, L., Tampieri, A., Sandri, M., Sprio, S.,** Biomimetic Mg-substituted hydroxyapatite: from synthesis to in vivo behavior. *J. Mater. Sci.: Mater. Med.,* 2008, vol. 19, pp. 239-247. http://dx.doi.org/10.1007/s10856-006-0032-y
4. **Matsunga, K.,** First-principles study of substitutional magnesium and zinc in hydroxyapatite and octacalcium phosphate. *The Journal of Chemical Physics*, 2008, vol. 128.
5. **Cacciotti, I., Bianco, A., Lombardi, M., Montanaro, L.,** Mg-substituted hydroxyapatite nanopowders: Synthesis, thermal stability and sintering behavior. *J. Eur. Ceram. Soc*., 2009, vol. 29, p. 2969-2978. http://dx.doi.org/10.1016/j.jeurceramsoc.2009.04.038
6. **Tardei, C., Grigore, F., Pasuk, I., Storleriu, S.,** The study of Mg^{2+}/Ca^{2+} substitution of β-tricalcium phosphate. *Journal of Optoelectronics and advanced Materials*, 2006, vol. 8, p. 568-571.
7. **Ren, F., Leng, Y., Xin, R., Ge, X.,** Synthesis, characterization and ab intio simulation of magnesium-substituted hydroxyapatite. *Acta Biomater.* , 2010, vol. 6, p. 2787-2796. http://dx.doi.org/10.1016/j.actbio.2009.12.044
8. **Kim, S.R., Lee, J.H., Kim, Y.T., Riu, D.H., Jung, S.J., Lee, Y.J., Chung, S.C., Kim, Y.H.,** Synthesis of Si, Mg substituted hydroxyapatites and their sintering behaviour. *Biomaterials*, 2003, vol. 24, p. 1389-1398. http://dx.doi.org/10.1016/S0142-9612(02)00523-9
9. **Laurencin, D., Barrios, N.A., de Leeuw, N.H., Gervais, C., Bonhommec, C., Mauri, F., Chrzanowski, W., Knowles, J.C., Newport, R.J, Wong, A., Gan, Z., Smith, M.E.,** Magnesium incorporation into hydroxyapatite. *Biomaterials,* 2011, vol.32, p. 1826-1837. http://dx.doi.org/10.1016/j.biomaterials.2010.11.017
10. **Mayer, I, Schlam, R, Featherstone, J.D.B.,** Magnesium-containing carbonate apatites. Journal of Inorganic Biochemistry, 1997, p. 1-6. http://dx.doi.org/10.1016/S0162-0134(96)00145-6

11. **Fadeev, I.V., Shvorneva, L.I., Barinov, S.M., Orlovskii, V.P.,** Synthesis and structure of magnesium-substituted hydroxyapatite**,** *Inorg. Mater.*, 2003, vol. 39, p. 947-950.
12. **Riman, R.E., Suchanek, W., Shuk, P., TenHuisen, K.S.,** Magnesium-substituted hydroxyapatites. US Patent 6921544 B2 (2005).
13. **Suchanek, W.L., Byrappa, K., Shuk, P., Riman, R.E., Janas, V.F., TenHuisen, K.S.,** Preparation of magnesium-substituted hydroxyapatite powders by the mechanochemical-hydrothermal method. *Biomaterials*, 2004, vol. 25, p. 4647-4657. http://dx.doi.org/10.1016/j.biomaterials.2003.12.008
14. **Landi, E., Tampieri, A., Mattioli-Belmonte, M., Celotti, G., Sandri, M., Gigante, A., Fava, P., Biagini, G.,** Biomimetic Mg- and Mg, CO-substituted hydroxyapatites: synthesis characterization and in vitro behavior. *J. Eur. Ceram. Soc.,* 2006, vol. 26, p. 2593-2601. http://dx.doi.org/10.1016/j.jeurceramsoc.2005.06.040
15. **Sanosh, K.P., Chu, M.-C., Balakrishan, A.,** Synthesis of nano hydroxyapatite powder that simulate teeth particle morphology and composition. *Curr. Appl. Phys.*, 2009, vol. 9, p. 1459-1462 http://dx.doi.org/10.1016/j.cap.2009.03.024
16. **Pena, J., Vallet-Regi, M.,** Hydroxyapatite, tricalcium phosphate and biphasic materials prepared by a liquid mix technique. *J. Eur. Ceram. Soc.*, 2003, vol. 23, p. 1687–1696. http://dx.doi.org/10.1016/S0955-2219(02)00369-2

Liga Stipniece, Mg.sc.ing., Research Assistant at the Institute of General Chemical Engineering, Riga Technical University. Main fields of interest include the synthesis and characterization of substituted HAp and the studies of HAp structural stability.
E-mail: liga.stipniece@rtu.lv

Kristine Salma-Ancane, Dr.sc.ing., Lecturer and Researcher at the Institute of General Chemical Engineering, the Faculty of Materials Science and Applied Chemistry, Riga Technical University. She is the author of more than 40 scientific publications in the branch of hydroxyapatite synthesis and characterization. Over the past 5 years, her scientific interest has been focused on the study of the influence of different technological parameters on physiochemical properties of hydroxyapatite bioceramics.
E-mail: kristine.salma-ancane(@rtu.lv

Dmitrijs Jakovlevs, Mg.sc.ing., Researcher at Rudolfs Cimdins Riga Biomaterials Innovation and Development Centre, Riga Technical University. He is a co-author of more than 20 scientific publications in the field of structural characterization of materials, such as biomaterials, clays, nanocomposites, TiO_2 ceramics etc. using the field emission scanning electron microscopy.
E-mail: Dmitrijs.Jakovlevs@rtu.lv

Natalija Borodajenko, Mg.sc.ing., Researcher at the Institute of General Chemical Engineering of Riga Technical University. She is an operator of Fourier transform infrared spectrometer and a co-author of more than 30 scientific publications.
E-mail: natalija.borodajenko@rtu.lv

Liga Berzina-Cimdina, Dr.sc.ing., a Professor, the Head of the Institute of General Chemical Engineering, Director of Rudolfs Cimdins Riga Biomaterials Innovation and Development Centre, and the Head of the Department of General Chemical Engineering at RTU, the Faculty of Materials Science and Applied Chemistry. She manages study programme specializations for: Chemistry and Technology of Biomaterials, Environmental Engineering, General Chemical Technology. Scientific research activities of Prof. L.Berzina-Cimdina include the management of international and regional projects (the EU, the Balkan countries, Latvia), development of new biomaterials and eco-materials, research of new applications for these materials and research on the interaction of materials and biological systems. She is the author of more than 100 scientific publications, as well as the author and a co-author of 3 patents.
E-mail: liga.berzina-cimdina@rtu.lv

Līga Stīpniece, Kristīne Šalma-Ancāne, Dmitrijs Jakovļevs, Natālija Borodajenko, Līga Bērziņa-Cimdiņa. Pētījumi par magnija iekļaušanās ietekmi uz hidroksilapatīta fizikālķīmiskajām īpašībām

Darba mērķis bija iegūt hidroksilapatīta biokeramiku ar variējamu Mg saturu. Mērķa sasniegšanai tika izvirzīti sekojoši uzdevumi - izstrādāt modificētu hidroksilapatīta sintēzes tehnoloģiju Mg saturoša reaģenta pievienošanai sintēzes vidē, kā arī (Mg^{2+}) jonu iekļaušanai sintēzes produktu struktūrā un izvērtēt (Mg^{2+}) jonu iekļaušanas efektivitāti un ietekmi uz hidroksilapatīta produktu īpašībām pēc sintēzes un termiskās apstrādes, veikt iegūto sintēžu produktu fāžu un molekulārā sastāva, kā arī morfoloģijas, mikrostruktūras pētījumus pēc sintēzes un termiskās apstrādes, kā arī veikt sintēžu produktu ķīmisko elementu koncentrācijas analīzi un termiskās stabilitātes pētījumus. Tika sintezēts ar Mg aizvietots hidroksilapatīts ar variējamu (0.21-4.72 masas%) Mg saturu, izmantojot modificētu šķīduma ķīmiskās nogulsnēšanas metodi no CaO, MgO un H_3PO_4. Pēc sintēzes un termiskās apstrādes ar Mg aizvietota hidroksilapatīta produktu rentgendifrakcijas ainās netiek detektētas tādas blakusfāzes kā $Mg(OH)_2$ un MgO, kas liecina par pilnīgu Mg jonu iekļaušanos hidroksilapatīta struktūrā. Lauka emisijas skenējošās elektronu mikroskopijas/enerģijas dispersīvās rentgenstaru spektroskopijas dati liecina, ka Mg koncentrācija sintēžu produktos pieaug līdz ar MgO daudzumu palielināšanu izejas $(Ca(OH)_2/Mg(OH)_2)$ suspensijā. Paaugstinoties iekļautā Mg daudzumam produktos, samazinās ar Mg aizvietota hidroksilapatīta termiskā stabilitāte, notiek daļēja fāžu transformācija uz ar Mg aizvietotu β-trikalcija fosfātu jeb vitlokītu. Hidroksilapatīta struktūrā iekļautais Mg būtiski izmaina to produktu kristalītu morfoloģiju un biokeramikas mikrostruktūru. Hidroksilapatītam raksturīga adatveida kristalītu aglomerātu morfoloģija, savukārt ar Mg aizvietotam hidroksilapatītam - plākšņveida kristalītu aglomerātu morfoloģija.

Лига Стипниеце, Кристине Салма-Анцане, Дмитрий Яковлев, Наталия Бородаенко, Лига Берзиня-Цимдиня. Изучение физико-химических свойств магний-замещенного гидроксиапатита

Целью работы было получение биокерамики гидроксиапатита с переменным содержанием Mg. Для достижения этой цели были определены задачи - разработать технологии синтеза Mg-замещенного гидроксиапатита, оценить эффективность ионного включения в структуре гидроксиапатита и оценить их влияние на характеристики продуктов гидроксиапатита, изучить фазовый и молекулярный состав продуктов синтеза, а также изучить морфологию, микроструктуру продуктов после синтеза и продуктов после термической обработки при высокой температуре (1100 градусов по Цельсию). Определить концентрацию химических элементов и изучить термическую стабильность биокерамики гидроксиапатита и биокерамики Mg-замещенного гидроксиапатита. Mg-замещенный гидроксиапатит с переменным количеством Mg (0.21-4.72 мас%), интегрированным в структуру, был синтезирован путем мокрого химического осаждения из CaO, MgO и H_3PO_4. Рентгеновский дифракционный анализ не показывает наличие $Mg(OH)_2$ и MgO в Mg-замещенных продуках после синтеза и термообработки, это указывает на полное включение Mg в структуру гидроксиапатита. Данные сканирующей электронной микроскопии/энергии дисперсионной рентгеновской спектроскопии указывают на то, что концентрация Mg в Mg-замещенном гидроксиапатите растет за счет увеличения содержания MgO в исходном $(Ca(OH)_2/Mg(OH)_2)$ растворе. Термическая стабильность Mg-замещенного гидроксиапатита уменьшается за счет увеличения количества Mg в продуктах, происходит частичное преобразование Mg-замещенного гидроксиапатита в Mg-замещенный β-трикальцийфосфат. Включение Mg в структуру гидроксиапатита существенно влияет на морфологию и микроструктуру. Для гидроксиапатита характерна морфология агломератов игольчатых кристаллитов, тогда как для Mg-замещенного гидроксиапатита - морфология агломератов пластинчатых кристаллитов.